Dermal reflectivity determined by optical coherence tomography is an indicator of epidermal hyperplasia and dermal edema within inflamed skin

Kevin G. Phillips
Yun Wang
David Levitz
Niloy Choudhury
Emily Swanzey
James Lagowski
Molly Kulesz-Martin
Steven L. Jacques

Dermal reflectivity determined by optical coherence tomography is an indicator of epidermal hyperplasia and dermal edema within inflamed skin

Kevin G. Phillips,[a,b,]* **Yun Wang,**[a] **David Levitz,**[d] **Niloy Choudhury,**[a,b] **Emily Swanzey,**[a] **James Lagowski,**[a] **Molly Kulesz-Martin,**[a,c] **and Steven L. Jacques**[a,b]

[a]Oregon Health and Science University, Department of Dermatology, 3303 S. W. Bond Avenue, Portland, Oregon 97239
[b]Oregon Health and Science University, Department of Biomedical Engineering, 3303 S. W. Bond Avenue, Portland, Oregon 97239
[c]Oregon Health and Science University, Department of Cell and Development Biology, 3303 S. W. Bond Avenue, Portland, Oregon 97239
[d]Tel-Aviv University, Department of Biomedical Engineering, Tel-Aviv, Israel 69978

Abstract. Psoriasis is a common inflammatory skin disease resulting from genetic and environmental alterations of cutaneous immune responses. While numerous therapeutic targets involved in the immunopathogenesis of psoriasis have been identified, the *in vivo* dynamics of inflammation in psoriasis remain unclear. We undertook *in vivo* time course focus-tracked optical coherence tomography (OCT) imaging to noninvasively document cutaneous alterations in mouse skin treated topically with Imiquimod (IMQ), an established model of a psoriasis-like disease. Quantitative appraisal of dermal architectural changes was achieved through a two parameter fit of OCT axial scans in the dermis of the form $A(x, y, z) = \rho(x, y) \exp[-\mu(x, y)z]$. Ensemble averaging over 2000 axial scans per mouse in each treatment arm revealed no significant changes in the average dermal attenuation rate, $\langle\mu\rangle$, however the average local dermal reflectivity $\langle\rho\rangle$, decreased significantly following 1, 3, and 6 days of IMQ treatment ($p < 0.001$) in comparison to vehicle-treated control mice. In contrast, epidermal and dermal thickness changes were only significant when comparing controls and 6-day IMQ treated mice. This suggests that dermal alterations, attributed to collagen fiber bundle enlargement, occur prior to epidermal thickness changes due to hyperplasia and dermal thickness changes due to edema. Dermal reflectivity positively correlated with epidermal hyperplasia ($r^2_{\text{epi}} = 0.78$) and dermal edema ($r^2_{\text{derm}} = 0.86$). Our results suggest that dermal reflectivity as measured by OCT can be utilized to quantify a psoriasis-like disease in mice, and thus has the potential to aid in the quantitative assessment of psoriasis in humans. © *2011 Society of Photo-Optical Instrumentation Engineers (SPIE)*. [DOI: 10.1117/1.3567082]

Keywords: optical coherence tomography; psoriasis; edema; dermatology.

*Address all correspondence to: Kevin Phillips, Dermatology Research, Oregon Health and Science University, 3181 SW Jackson Park Road-L468R, Portland, Oregon 97210. E-mail: phillkev@ohsu.edu.

1 Introduction

Psoriasis is a chronic inflammatory skin disease that affects 2 to 3% of the population worldwide. The etiology of psoriasis is unclear, although it is known that both genetic and environmental factors influence disease formation and severity. Patients present with pruritic, erythematous, scaly plaques that can occur in either limited or widespread areas of the body. Significant morbidity often results in patients with lesions occurring in sensitive areas, such as the palms, soles, or genitalia, when lesions are generalized, and/or in those individuals with concomitant psoriatic arthritis.

Previous studies have revealed that skin affected by psoriasis involves a complex inflammatory network of cytokines, chemokines, and growth factors produced by a variety of cell types, including T cells, dendritic cells, keratinocytes, dermal fibroblasts, as well as blood and lymphatic endothelial cells.[1] This pathogenic process results in hyperplasia of the epidermis, infiltration of leukocytes into the dermis and epidermis, and dilation and growth of blood vessels. In spite of this understanding, the *in vivo* dynamics of the immunopathogenesis of psoriasis remain unclear. *In vivo* optical imaging modalities have the potential to provide quantitative morphological appraisal of affected tissues in order to understand the spatial-temporal evolution and molecular dependence of disease progression and abatement.[2–4]

Clinical investigations of psoriasis utilizing optical coherence tomography (OCT) imaging, a noninvasive interferometric optical imaging modality capable of imaging distinct skin layers up to 2 mm in depth, have recently demonstrated the correlation of OCT derived epidermal thickness measurements with the psoriasis area and severity index.[3] In separate investigations of cancerous tissues, parametric models of OCT axial attenuation and reflectivity properties have demonstrated unique optical signatures specific to normal and cancerous tissue architectures.[5,6] We hypothesized that the immunopathogenesis of psoriasis affects dermal architecture in a similarly measurable way, thus providing the potential to monitor this disease through unique properties inherent to OCT axial scans through involved tissues under investigation.

In this letter, we demonstrate a simple two parameter model to elucidate intrinsic features of raw OCT data capable of characterizing psoriasis-like inflammation in the skin of mice in terms of epidermal thickness changes and unique reflectivity signatures associated with structural reorganization of collagen fibers in the dermis of involved tissues. Thus, parametric models of OCT images can be deployed to investigate tissue responses to new therapeutic targets in animal models as well as aid in the realtime noninvasive OCT-based evaluation of psoriasis severity in clinical settings.[3,4,7]

2 Materials and Methods

Imiquimod (IMQ) is an immune activator used for topical treatments of human papilloma virus associated warts and precancerous skin lesions including actinic keratoses and superficial

basal cell carcinomas. IMQ has also been shown to exacerbate psoriasis symptoms in psoriatics treated for skin cancers[8] and has recently been demonstrated to induce psoriasis-like skin inflammation in mice along the IL-23/IL-17 axis,[9] making IMQ treatment a novel animal model of the human disease.

Wild type (WT) and heterozygous K14.Trim32 transgenic (K14.Trim32 Tg) mice on a DBA2/C57BL6 background were treated on the inner side of the ear flap (to avoid scratching) with a daily topical dose of 62.5 mg of IMQ cream (5%) (Aldera; 3M Pharmaceuticals) for 1, 3, and 6 days.[9] A control group (3 mice per strain) was treated similarly for 6 days with Aquaphor (Eucerin) vehicle. Time-domain focus-tracked OCT imaging at 1310 nm with axial resolution of $\sim$7.8 μm and lateral resolution of $\sim$6.3 μm (in air)[10] was carried out on 6 mice each (3 mice per strain) at days 1, 3, and 6. Vehicle-treated mice were imaged on the 6th day of treatment. Mice were anesthetized with isoflourine (1.5% V/V at 1 ATM) and placed in the supine position to enable imaging of the inner side of the ear flap. Ears were optically coupled to a mirror with optical gel (GenTeal; Novartis) to serve as a visual aid in OCT sagittal scans. A tissue volume of 300 μm$\times$15 μm$\times$1000 μm (2000 axial scans) in the central region of each ear was optically interrogated at a rate of $\sim$50 axial scans per second. Ten axial scans were acquired at each location to average out speckle noise, making the total acquisition time 6 to 7 min per mouse.

Figure 1 illustrates the morphological differences observed in hematoxylin and eosin stains of 6-day cream controls [Fig. 1(a)], and 6-day IMQ treatments [Fig. 1(b)]. A thicker epidermis and dermis and increased cellularity of the dermal and epidermal compartments can be appreciated in the IMQ model of psoriasis-like inflammation [Fig. 1(b)]. Similar enlargement of the epidermis and dermis are observed in the corresponding OCT sagittal scans [Figs. 1(c) and 1(d)]. In all panels of
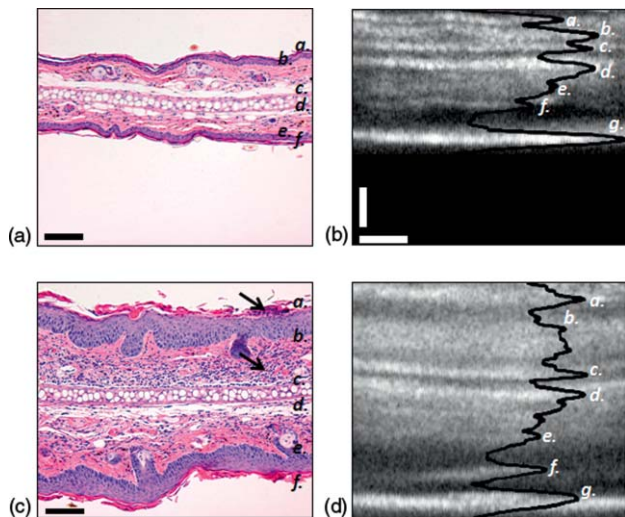

Fig. 1 Altered cell proliferation/differentiation/infiltration of ear tissue after 6-day IMQ treatment. (a) H&E stain of cream control and (b) 6-day IMQ treatment; black arrows indicate nucleated immune cell infiltrate into the epidermis and dermis. Scale bars denote 100 μm. (c), (d) Corresponding focus-tracked OCT sagittal scans (average of 10 B-scans taken at the same location, with histogram adjustment) and axial scan overlay in solid black. Scale bars: vertical 100 μm, horizontal 50 μm. In all images (a,f) denotes the stratum corneum; (b,e) denote the dermis; (c,d) denote the borders of the cartilage layer running through the center of the ear. In the OCT images, (g) denotes the mirror.
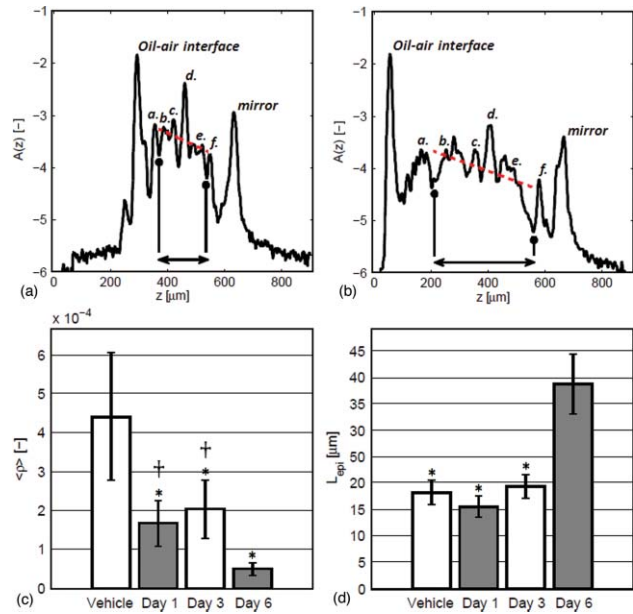

Fig. 2 Quantitative appraisal of IMQ induced skin reorganization using OCT axial scans. Axial profile (log base 10 scale) of (a) control and (b) 6-day IMQ treated DBA2/C57BL6 mouse ears. Arrows in (a) and (b) denote the upper and lower dermis of the ear, utilized in the parametric fit (dotted line) of the form $\rho \exp(-\mu z)$. (c) Bar graph indicating the decrease of the ensemble averaged dermal reflectivity, $\langle\rho\rangle$, in response to daily IMQ treatment in mouse ear. (*) indicates $p < 0.05$ in comparison to control, (†) indicates $p < 0.05$ in comparison to 6-day IMQ treatment. (d) Bar graph indicating epidermal thickness, (*) indicates $p < 0.05$ in comparison to 6-day IMQ treated ears. In panels (a) and (b): (a,f) denotes the stratum corneum; (b,e) denote the dermis; (c,d) denote the borders of the cartilage layer running through the center of the ear.

Fig. 1, (a) and (f) indicate the stratum corneum, (b) and (e) indicate the dermis, and (c) and (d) denote the borders of the cartilage layer running through the center of the ear. The dermal-epidermal junction (DEJ) in the OCT sagittal scans is the dark region occurring between (a) and (b) and (e) and (f). The DEJ appears dark as a result of forward scattering by this highly nucleated region of the tissue. Epidermal thickness was determined for the inner ear using the distance between the stratum corneum and the DEJ. This corresponds to taking the axial distance between the first peak to the first valley in the axial scans.[11] Dermal thickness was taken to be the distance between the dorsal and ventral DEJs, thus including the cartilage layer. The bottom bright layer, denoted as (g) in Figs. 1(c) and 1(d), is the mirror upon which the ear was imaged.

For each position $\mathbf{r} = (x, y)$ on the tissue surface, a two parameter model of the form $A(\mathbf{r}, z) = \rho(\mathbf{r})\exp[-\mu(\mathbf{r})z]$, is fit to the raw OCT axial scans. The fit is performed over the range of axial depths beginning at the dorsal DEJ of the ear and ending at the ventral DEJ, the indicated region in Figs. 2(a) and 2(b). The local dermal reflectivity fit parameter $\rho(\mathbf{r})$ is converted from detector units to dimensionless reflectance units through multiplication by a calibration factor, $C = R_{\text{air.oil}}/D$, defined as the ratio of the reflected intensity at an air-oil interface (assuming normal incidence), $R_{\text{air.oil}}$, to the corresponding detector unit, D [a.u.]. Here $C = 0.031$ [dimensionless reflectance units/detector units]. $\mu(\mathbf{r})$ [μm^{-1}] fits the average dermal attenuation rate, slope of the dotted line in Figs. 2(a) and 2(b).

Ensemble averages and standard deviations of the fit parameters and epidermal/dermal thickness values were determined for 2000 axial scans comprising the image cube for each animal in each treatment arm of the study. Statistical significance of the fit parameters and thickness variations with treatment was assessed using one way analysis of variance with Bonferonni *post hoc* analysis performed on all treatment groups; *p*-values less than 0.05 after a Bonferroni post-test were considered statistically significant. In all instances data are presented as mean ± standard deviation.

3 Results

There was no statistically significant strain dependence (WT versus K14.Trim32 Tg) to the IMQ induced inflammation. All values are reported as the combined average of 3 WT and 3 K14.Trim32 Tg mice at each time point.

The epidermis increased in thickness from 18.2±2.5 μm in control mice to 38.8±5.8 μm in the 6-day IMQ treatment group ($p = 0.0001$) [Fig. 2(d)]. The thickness of the dermal region increased from 193.9±37.4 μm in control mice to 383.9 ±43.8 μm ($p = 0.0001$). These results were in keeping with previous reports of IMQ induced hyperplasia and dermal immune cell infiltrate.[9] No statistically significant increase in the thickness of the epidermis or dermis was observed in 1- and 3-day IMQ treatment groups in comparison to vehicle-treated controls.

In contrast, local dermal reflectivity decreased in a significant way when comparing all IMQ treatment time points to vehicle controls [Fig. 2(c)]. Statistically significant differences in dermal reflectivity were also found when comparing 1- and 6-day treatment groups ($p = 0.0019$) and 3- and 6-day treatment groups ($p = 0.0022$). These results suggest that architectural changes in the dermis occur before keratinocyte proliferation in the epidermis and swelling of the dermis. Reductions in local dermal reflectivity were positively correlated with dermal swelling ($r^2_{\mathrm{derm}} = 0.86$) and epidermal hyperplasia ($r^2_{\mathrm{epi}} = 0.78$).

No statistically significant separation in the average dermal attenuation, μ, was observed. Previous investigations[12] of the μ and ρ fitting variables of the parametric model utilized in this study and their connection to the optical properties of light transport theory (scattering coefficient, μ_s, and anisotropy factor, g) indicate that an unchanging μ and decreasing ρ correspond to a slight increase in μ_s and a significant increase in g. Based on a Mie theory analysis of μ_s and g[12] scattering constituents in the dermis must increase in size to mitigate an increase in g with little change in μ_s. We thus conjecture that collagen fiber bundles in the dermis must swell in response to the presence of edematous fluid infiltrate preceding dermal swelling.

4 Conclusions

Dermal reflectivity was found to decrease with increasingly severe psoriasis-like inflammation in mouse skin. No significant alteration in μ was observed. This comes into contrast with decreased attenuation of OCT axial scans observed in psoriasis and contact dermatitis involved skin in humans.[4] With no corresponding ρ results in the human studies, it is difficult to separate the effects of scattering coefficient and scattering anisotropy on attenuation and reflectivity to infer possible size changes in the scattering constituents dur-

ing inflammation. Alternatively, the distinct physiology of the mouse ear, most notably the highly reflective cartilage layer, might also influence the fit parameters that inform our analysis. Nevertheless, our results in mice demonstrate that the positive correlation of the OCT fit parameter ρ to epidermal/dermal thickness changes and the theoretical connection of both μ and ρ to the size of scattering constituents in the tissue provide a label-free OCT based *in vivo* quantification of inflammation. These parameters can be readily translated to the realtime clinical appraisal of psoriatic lesions in humans. In the clinic, dermal reflectivity can potentially serve as a complementary grading system of disease severity that can be used in conjunction with the psoriasis area and severity index to monitor patient disease and therapeutic efficacy.

1. E. F. Wagner, H. B. Schonthaler, J. Guinea-Viniegra, and E. Tschachler, "Psoriasis: What we have learned from mouse models," *Nat. Rev. Rheumatol.* **6**(12), 704–714 (2010).
2. H. L. Rizzo, S. Kagami, K. Phillips, S. E. Kurtz, S. Jacques, and A. Blauvelt, "Il-23-mediated psoriasis-like epidermal hyperplasia is dependent upon il-17a," *J. Immunol.* **186**(3), 1495–1502 (2011).
3. H. Morsy, S. Kamp, L. Thrane, N. Behrendt, B. Saunder, H. Zayan, E. A. Elmagid, and G. B. E. Jemec, "Optical coherence tomography imaging of psoriasis vulgaris: Correlation with histology and disease severity," *Arch. Dermatol. Res.* **302**, 105–111 (2010).
4. J. Welzel, M. Bruhns, and H. H. Wolff, "Optical coherence tomography in contact dermatitis and psoriasis," *Arch. Dermatol. Res.* **295**, 50–55 (2003).
5. R. A. McLaughlin, L. Scolaro, P. Robbins, C. Saunders, S. L. Jacques, and D. D. Sampson, "Parametric imaging of cancer with optical coherence tomography," *J. Biomed. Opt.* **15**, 046029 (2010).
6. P. Tomlins, O. Adegun, E. Hagi-Pavli, K. Piper, D. Bader, and F. Fortune, "Scattering attenuation microscopy of oral epithelial dysplasia," *J.Biomed. Opt.* **15**(6), 066003 (2010).
7. M. Ardigo, C. Cota, E. Berardesca, and S. Gonzalez, "Concordance between *in vivo* reflectance confocal microscopy and histology in the evaluation of plaque psoriasis," *J. Eur. Acad. Dermatol. Venereol.* **23**(6), 660–667 (2009).
8. N. Rajan and J. Langtry, "Generalized exacerbation of psoriasis associated with imiquimod cream treatment of superficial basal cell carcinomas," *Clin. Exp. Dermatol.* **31**, 140–141 (2006).
9. L. van der Fits, S. Mourits, J. S. Voerman, M. Kant, L. Boon, J. D. Laman, F. Cornelissen, A.-M. Mus, E. Florencia, E. P. Prens, and E. Lubberts, "Imiquimod-induced psoriasis-like skin inflammation in mice is mediated via the il23/il-17 axis," *J. Immunol.* **182**(9), 5836–5845 (2009).
10. N. Choudhury, G. Song, F. Chen, S. Matthews, T. Tschinkel, J. Zhen, S. L. Jacques, and A. L. Nuttall, "Low coherence interferometry of the cochlear partition," *Hear. Res.* **220**, 1–9 (2006).
11. T. Gambichler, G. Moussa, P. Regeniter, C. Kasseck, M. Hoffmann, F. Bechara, M. Sand, P. Altmeyer, and K. Hoffmann, "Validation of optical coherence tomography *in vivo* using cyrostat histology," *Phys. Med. Biol.* (**52**), N75–N85 (2007).
12. R. Samatham, K. G. Phillips, and S. L. Jacques, "Assessment of optical clearing agents using reflectance mode confocal scanning laser microscopy," *JIOHS* **3**(3), 183–188 (2010).